

REVIEW

The super-LHC (To appear in Contemporary Physics)

Michelangelo L. Mangano^{a*}

^a*CERN, PH-TH, 1211 Geneva 23, Switzerland;*

We review here the prospects of a long-term upgrade programme for the Large Hadron Collider (LHC), CERN laboratory's new proton-proton collider. The super-LHC, which is currently under evaluation and design, is expected to deliver of the order of ten times the statistics of the LHC. In addition to a non-technical summary of the principal physics arguments for the upgrade, I present a pedagogical introduction to the technological challenges on the accelerator and experimental fronts, and a review of the current status of the planning.

Keywords: particle physics; hadronic collisions; accelerators; LHC; CERN

1 Introduction

The Large Hadron Collider (LHC) is the new particle accelerator about to start taking data at CERN's laboratory. It will collide protons against each other, at a centre-of-mass energy of 14 TeV. Its primary goal is to answer one of the deepest questions of physics today, namely what is the origin of the elementary particles' masses. In particular, it should be able to verify whether the mechanism postulated by the current theory of particle physics, the Standard Model [1, 2, 3, 4], is correct, or whether this requires additional ingredients.

The Standard Model, whose complete formulation dates back to the early 70's, has been shown over the past 30 years to accurately describe all properties of the interactions among fundamental particles, namely quarks, leptons and the gauge bosons transmitting the electroweak and strong forces [5, 6, 7]. Its internal consistency, nevertheless, relies on a mechanism to break the symmetry between electromagnetic and weak interactions, the so-called electroweak symmetry breaking (EWSB).

EWSB is a necessary condition for elementary particles to acquire a mass. The reason is that weak interactions have been shown experimentally, since the 50's, to be *chiral*, namely to behave differently depending on whether the projection of a particle spin along its momentum points towards the direction of motion (positive chirality) or against (negative chirality). Since the chirality of a massive particle can change sign by changing Lorentz reference frame, the weak charge of a massive particle cannot commute with the Hamiltonian, and the associated symmetry must be broken. The simplest way to achieve this [2] is to assume the existence of a scalar field with a weak charge, the Higgs H , whose potential energy is minimized with a non-vanishing value of its matrix element on the vacuum state, $\langle H \rangle = v \neq 0$. This leads to spontaneous symmetry breaking. The measured strength of the weak interactions and the mass of their carriers, the W^\pm gauge bosons, fix the value of $v \sim 247$ GeV, thus setting the natural mass scale for weak phenomena.

*Email: michelangelo.mangano@cern.ch

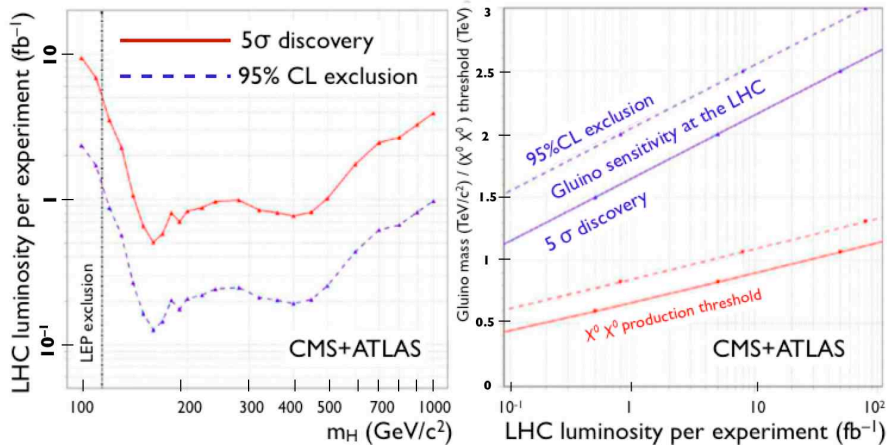


Figure 1. Discovery reach and exclusion limits at the LHC for a Standard Model Higgs (left) and for gluinos in a supersymmetric theory (right), as a function of the integrated luminosity [11].

The fluctuations of the Higgs field around its vacuum state give rise to a particle, the Higgs boson, whose mass m_H is a free parameter of the model. Direct searches at the LEP e^+e^- collider have established a lower limit $m_H \gtrsim 114$ GeV, important constraints in the mass range around 170 GeV have been recently achieved by the Tevatron experiments [8], and theoretical analyses of the consistency of the model set an upper limit, around 800 GeV. The design of the LHC collider and of its two largest experiments, ATLAS [9] and CMS [10], has been tuned to enable the full exploration of this mass range, searching for a broad variety of the Higgs production and decay processes predicted by the Standard Model.

The timeline for these searches is outlined in the left plot of fig. 1, taken from [11]. This shows the amount of data, needed by each of the two experiments to establish a 5σ discovery, or a 95%CL exclusion, as a function of the Higgs mass. The present planning of LHC operations foresees the delivery of a few 100 pb^{-1} of data during the first year, and of the order of 1–few fb^{-1} over the next couple of years at a luminosity of about $10^{33} \text{ cm}^{-2}\text{s}^{-1}$. After reaching the *nominal* luminosity of $10^{34} \text{ cm}^{-2}\text{s}^{-1}$, the LHC should start delivering about 60 fb^{-1} per year, when accounting for down-time and running efficiency.

A comparison with fig. 1 therefore shows that, within 2–3 years of data taking, the Standard Model Higgs boson will be discovered, or entirely excluded, over the full mass range. In either case, this will signal the beginning, rather than the completion, of the LHC physics programme. Should the Higgs boson be found, an extensive campaign of studies of its detailed properties will be required, to confirm that they match the expectations of the Standard Model, or to detect possibly minor deviations, unveiling a framework for EWSB more elaborate than the minimal one postulated by the Standard Model. If the Higgs boson is not found, a radical departure from the Standard Model will be needed, and the searches to understand what other mechanism is responsible for EWSB will begin.

The LHC experiments are designed to be able to tackle these further challenges, and the accelerator must be in the position to continue delivering larger and larger amounts of data to allow them to pursue this target. The goal of this review is to outline the potential of the LHC to further push the study of EWSB and the search for other new phenomena beyond the Standard Model (BSM), and to summarize the technological challenges that this entails, both in the development of a long-term higher-luminosity phase of the LHC accelerator, the super-LHC (sLHC), and in the upgrade of the detectors, to allow them to operate under the extreme experimental conditions that such a higher luminosity will create. The first part of this review will focus on the physics goals, discussing the possible measurements aimed at more firmly establishing the nature of the EWSB and at probing other new phenomena, and indicating the improvements that can be obtained by extending the LHC operations to data samples a factor of 10 larger than what is currently foreseen by the base programme. A few remarks will be included

on the impact of an energy upgrade of the LHC. The second part will discuss the possible evolution of the accelerator complex to deliver 10 times the luminosity, including a pedagogical overview of the main accelerator physics concepts required to appreciate the challenge. A third part will address the experimental constraints and the progress foreseen for the detectors.

A summary of the expectations for the first two years of measurements at the LHC can be found in [12]. The first complete discussion of the physics potential of the sLHC has been presented in [13]. Most of the results shown here are taken from this document: while in the ensuing years new theoretical ideas and new studies of the experimental prospects have appeared, the examples discussed here well illustrate the potential of the LHC, the main difficulties inherent in the analyses, and the added value provided by the sLHC. The first technical assessment of the feasibility of the accelerator upgrade is documented in [14]. The discussion presented here is based on the latest upgrade plans, and more details can be found in [15] and in [16], an excellent series of introductory lectures to be subject.

2 The physics potential of the LHC programme

As discussed in the introduction, the confirmation and exploration of the mechanism driving the electroweak symmetry breaking is today the main priority of particle physics. The Standard Model defines without ambiguity the mechanism which brings the Higgs boson to existence. There are nevertheless good reasons for theorists to suspect that physics *beyond* the Standard Model should play a key role in the dynamics of EWSB [17]. To start with, one would like to have a framework within which the smallness of the weak scale $v \sim 247$ GeV, relative to the Planck scale $M_{Pl} \sim 10^{19}$ GeV, is the natural result of dynamics, as opposed to a random accident. Furthermore, there are unequivocal experimental indications that BSM phenomena are required to explain what is observed in the universe: the Standard Model can explain neither the existence of dark matter [18], nor the ratio of baryons and radiation present in the universe. In addition, although neutrino masses could be incorporated with a minimal and trivial adjustment of the Standard Model spectrum, the most compelling explanations of how neutrinos acquire such a small mass rely on the existence of new phenomena at scales of the order of the Grand Unification, $M_{GUT} \sim 10^{15}$ GeV [19]. Furthermore, there are several questions that within the Standard Model cannot be addressed, but that could acquire a dynamical content in a broader framework. As an example, consider the issue of what is the origin of the three quark and lepton generations and of the diverse mass patterns between and within them. Since EWSB is ultimately responsible for the generation of masses, with the differentiation between flavours and the consequent appearance of mixing angles and CP violation, speculating a relation between EWSB and the flavour structure of the fundamental particles is unavoidable. This relation is trivial in the context of the Standard Model, where the flavour structure is determined by the couplings with the Higgs field, which are free, arbitrary, parameters. By contrast, in most BSM models the low-energy flavour structure emerges from a specific dynamics, and relations between masses and mixings of different particles are in principle calculable.

EWSB therefore brings together the two main elements of the Standard Model, the gauge and the flavour sectors. Their current theoretical description has so far survived the most stringent experimental tests, but both components are vulnerable, and liable to crack under the weight of new data. The various BSM proposals anticipate new phenomena to appear at the TeV mass scale: supersymmetry [20, 21], which implies the existence of a new boson for each fermionic particle of the Standard Model, and of a new fermion for each known boson; new forces, mediated by heavy gauge bosons, possibly restoring at high energy the chiral left-right asymmetry of the low-energy world; new strong interactions and new fermions, responsible for the dynamical generation of EWSB; compactified space dimensions, leading to the existence of an infinite Kaluza-Klein spectrum of particles corresponding to each known one, with ever increasing and linearly-spaced masses; composite structures within what are considered as fundamental, elementary particles; and more, with a continuous emergence of new ideas and proposals to embed

the Standard Model into a more complete theory. The LHC will be the first accelerator operating at energies high enough to explore a large fraction of these proposals. This section will present a few examples of the LHC discovery potential and of the benefits of a luminosity upgrade. They are just meant as illustrative, and a more detailed account is documented in ref. [13].

In addition to ATLAS and CMS, four other approved experiments will contribute to the completion of the LHC physics programme: ALICE [22], dedicated to the study of relativistic heavy ion collisions; LHCb [23], dedicated to the study of the properties of b -flavoured hadrons; TOTEM [24], dedicated to the measurement of total and elastic cross sections and LHCf [25], dedicated to the study of inclusive forward photon and π^0 spectra. None of these experiments will be engaged in the operations at the highest luminosities delivered by the sLHC, and this review will primarily focus on the issues relevant to the physics programme of ATLAS and CMS.

2.1 The Higgs sector and EWSB

As shown in fig. 1, the discovery of the Standard Model Higgs boson should be achievable by ATLAS and CMS independently with luminosities in the range of 10 fb^{-1} for the full mass range $114 < m_H \lesssim 800 \text{ GeV}$, and already with $\sim 1 \text{ fb}^{-1}$ in the regions around 160 and 400 GeV, where the $H \rightarrow ZZ^{(*)} \rightarrow 4$ leptons decay mode provides a very clean signal. Following the discovery, the main focus will become the quantitative study of the Higgs properties. The goal will be to establish whether it behaves as expected in the Standard Model, or whether BSM physics is present. Contrary to the rather generic expectation that the LHC will detect the Higgs, the issue of its precise nature is more open, as different BSM theories make different predictions for the precise nature of the EWSB mechanism. In some cases it will be straightforward to establish the incompatibility of the detected Higgs with the Standard Model. For example, a value of $m_H \gg 200 \text{ GeV}$ would clash with the result of electroweak fits. Likewise, a production cross-section significantly different from what is calculated would be a sign that either the couplings are different than expected, or that new states exist affecting the decay branching ratios, or both. Even a Higgs in the right mass range and with production rates roughly compatible with the Standard Model may still hide some underlying BSM dynamics [26], which could become evident once more accurate measurements become available. What is certain is that in this phase there will be no limit to the need for accuracy and thus for data statistics.

2.1.1 Determination of Higgs couplings

The expected precision in the determination of the Higgs couplings to fermions and gauge bosons is shown in fig. 2 [13, 27]. Model-independent results are given in terms of ratios of couplings. These are less prone to theoretical or experimental systematics, and are sufficient to exhibit possible deviations from the Standard Model, which could be rather large in many BSM scenarios, such as supersymmetry. The limited improvement with the sLHC luminosity of some of these measurements is due to the very conservative detector-performance assumptions made in [13]. This is to be reviewed in the near future, with more realistic studies.

Higher luminosity will allow the measurements of decays that would otherwise be too rare. An example is $H \rightarrow Z\gamma$, which in the mass region 115-160 GeV is predicted to have a branching ratio of a few $\times 10^{-3}$. The expected significance for 600 fb^{-1} (300 fb^{-1} per experiment) is $\sim 3.5 \sigma$ [13], to become $\sim 11 \sigma$ with a tenfold luminosity increase. In the case of $H \rightarrow \mu^+\mu^-$, the Standard Model branching ratio is of order 10^{-4} in the range 115-140 GeV, and the significance for 600 fb^{-1} is below 3σ , increasing to about 7σ at the sLHC [28].

2.1.2 Observation of extended Higgs sectors

Most BSM theories require the existence of more Higgs particles in addition to the excitation of the field responsible for EWSB. For example, in supersymmetry there are two Higgs doublets, one coupled to the up-type quarks, and one to the down-type quarks and to charged leptons. After EWSB, 3 Higgs fields emerge in addition to the Standard Model one, for a total of two CP-even (h^0 and H^0), one CP-odd (A^0) and one charged (H^\pm). The spectrum and couplings of

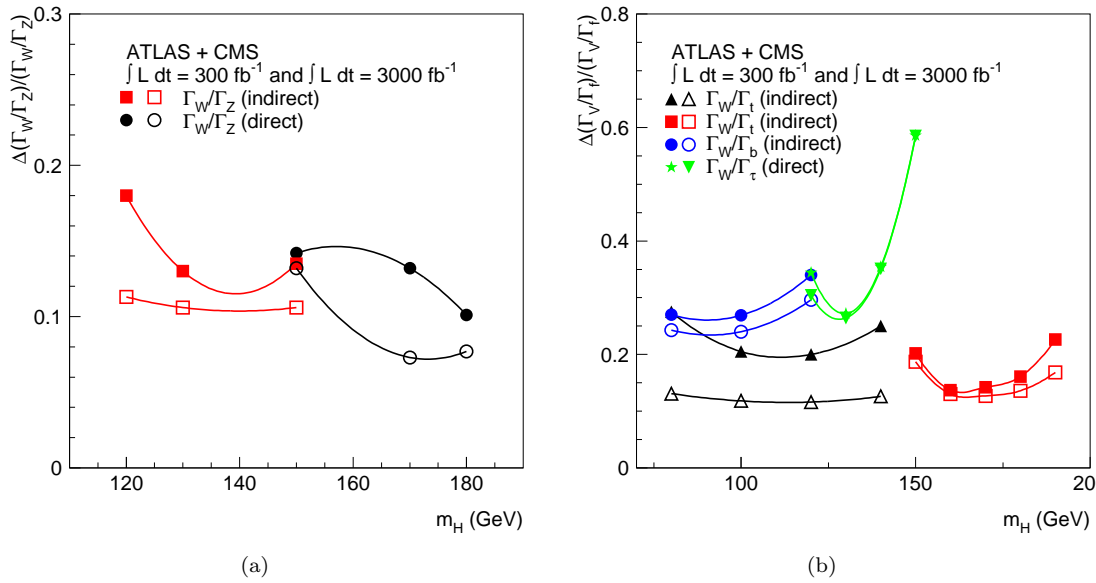


Figure 2. Expected uncertainties on the measured ratios of the Higgs widths to final states involving bosons only (a) and bosons and fermions (b), as a function of the Higgs mass. Closed symbols: two experiments and 300 fb^{-1} per experiment (standard LHC); open symbols: two experiments and 3000 fb^{-1} per experiment (sLHC). Direct and indirect measurements have been included.

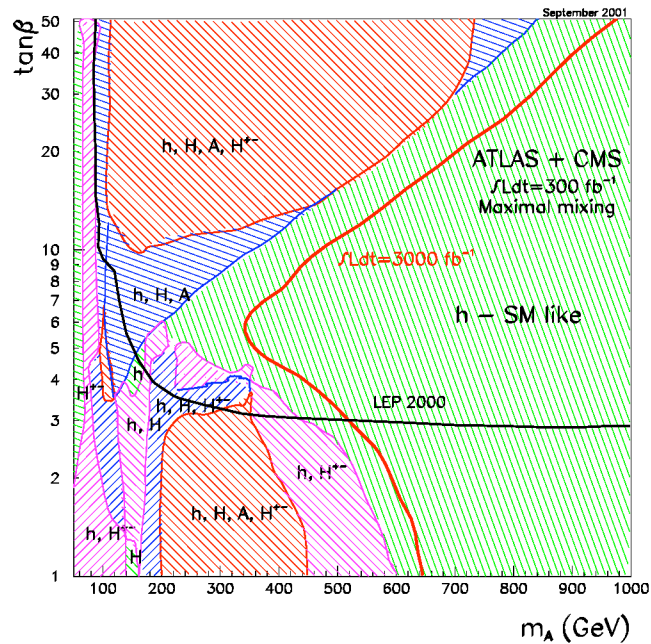


Figure 3. Regions of the MSSM parameter space where the various Higgs bosons can be discovered at $\geq 5\sigma$ at the LHC (for 300 fb^{-1} per experiment and both experiments combined) through their decays into Standard Model particles. In the region to the left of the rightmost contour at least two Higgs bosons can be discovered at the SLHC (for 3000 fb^{-1} per experiment and both experiments combined).

these states are determined by the parameters m_A (the mass of the CP-odd Higgs) and $\tan\beta$ (the ratio of expectation values of the neutral components of the two Higgs doublets). The measurement of these masses and couplings provides valuable information on the mechanism of supersymmetry breaking. The LHC discovery potential for additional Higgs bosons in the minimal supersymmetric standard Model (MSSM) is summarised in Fig. 3 [13]. Different shadings flag regions where different combinations of Higgs bosons can be discovered. This plot shows

that over a good part of the parameter space the LHC should be able to discover two or more Higgs bosons, except in the region at large m_A (the so-called “decoupling limit”). In this region, only the lightest Higgs boson h can be observed, unless the heavier Higgs bosons (H , A , H^\pm) have detectable decay modes into supersymmetric particles. This means that the LHC cannot promise a complete and model-independent observation of the heavy part of the MSSM Higgs spectrum, although the observation of sparticles (e.g. squarks and gluinos) will indicate that supersymmetry exist, and tell implicitly that additional Higgs bosons should exist. Figure 3 also shows that the sLHC should be able to extend significantly the region over which at least one heavy Higgs boson can be discovered at $\geq 5\sigma$ in addition to h (rightmost contour in the plot).

2.1.3 Strongly-coupled vector bosons

General arguments imply that [29], in absence of a Higgs boson below $m_H \sim 1$ TeV, the scattering of electroweak gauge bosons at high energy will show structure beyond that expected in the Standard Model: resonances, or other phenomena, must appear as a result of the strongly-interacting Higgs dynamics and to correct the breakdown of unitarity of the scattering amplitudes. Most recently, it has been pointed out [26] that such phenomena could also occur if the Higgs were light, should the Higgs be non-elementary, as in models where EWSB is induced by a high-energy strongly-interacting sector.

In order to explore such signals it is necessary to measure final states containing pairs of gauge bosons with invariant masses in the TeV range and above. The example given here refers to production of WZ pairs, in a chiral lagrangian model [30] in which the unitarization of the scattering amplitude in the absence of a Higgs boson is enforced by the presence of a massive vector resonance. Figure 4 shows the expected signal for a 1.5 TeV resonance, at the LHC and at the sLHC, after applying very strict analysis cuts to reduce the otherwise overwhelming QCD backgrounds [13]. At the LHC one requires the presence of a forward and a backward jet (namely jets with $|\eta| > 2^1$), with energies greater than 300 GeV, and the absence of central ($|\eta| < 2$) jets with transverse energy $E_T > 50$ GeV. At the sLHC, as discussed in section 4.1, the high luminosity leads to a large number of parasitic pp collisions overlapping with the primary interaction (the so-called pile-up events), and the associated released energy would promote background events into the signal region. One is therefore forced to tighten these cuts to 400 and 70 GeV, respectively, thus reducing in parallel the signal efficiency. The resonance is at the limit of the observability at the LHC, with 6.6 events of signal (S) expected over a background (B) of about 2.2 events around the region of the peak. At the sLHC, on the other hand, the signal has a significance of $S/\sqrt{B} \sim 10$. This example underscores the importance of keeping the number of pile-up events as small as possible, and of maintaining a good efficiency for reconstruction of forward jets, two of the driving requirements for the accelerator and the detector upgrades.

2.1.4 Gauge boson self-couplings

A further crucial test of models for EWSB is the precise measurement of the self-couplings of the electroweak gauge bosons. The Standard Model radiative corrections modify the Born-level results at the level of per mille, setting the goal for precision measurements. Table 1 [13] shows, for the CP-conserving anomalous couplings of the electroweak (EW) bosons, the accuracy expected with different options of luminosity and energy for the LHC, as well as with a low-energy linear collider [31]. Notice that here the tenfold increase in luminosity is more powerful than a twofold increase in energy at constant luminosity. The reason is that the growth in the production rates for pairs of gauge bosons is only logarithmic with beam energy, due to their rather low mass in relation to the available phase-space, and higher luminosity is therefore statistically more effective than higher energy.

¹The pseudorapidity η is related to the scattering angle θ by the relation $\eta = -\log \tan \theta/2$.

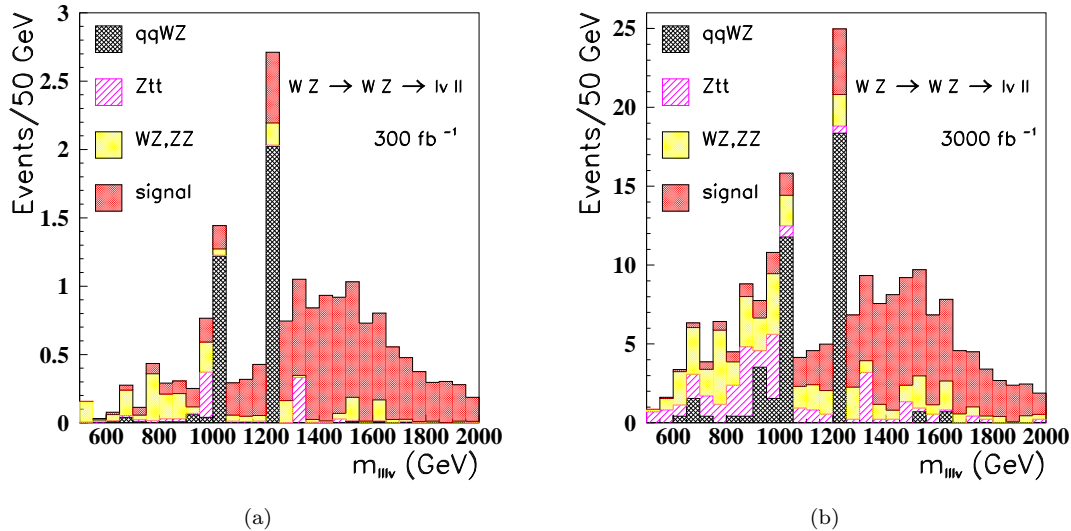


Figure 4. Expected signal and background for a 1.5 TeV WZ resonance in the leptonic decay channel for 300 fb^{-1} (a) and 3000 fb^{-1} (b).

Table 1. Expected accuracies for the CP-conserving anomalous couplings of EW gauge bosons. The last column refers to an e^+e^- linear collider (LC).

Coupling	14 TeV 100 fb^{-1}	14 TeV 1000 fb^{-1}	28 TeV 100 fb^{-1}	28 TeV 1000 fb^{-1}	LC (500 GeV) 500 fb^{-1}
λ_γ	0.0014	0.0006	0.0008	0.0002	0.0014
λ_Z	0.0028	0.0018	0.0023	0.009	0.0013
$\Delta\kappa_\gamma$	0.034	0.020	0.027	0.013	0.0010
$\Delta\kappa_Z$	0.040	0.034	0.036	0.013	0.0016
g_1^Z	0.0038	0.0024	0.0023	0.0007	0.0050

2.2 Supersymmetry

The current mass limits on supersymmetric particles reach 300–400 GeV, from the searches at the Tevatron collider [7]. As shown in fig. 1, few 100 pb^{-1} will be sufficient at the LHC to extend the 5σ sensitivity up to well above the TeV scale! The figure also shows that the mass sensitivity grows logarithmically with the statistics, with each new decade in integrated luminosity increasing the discovery reach by about 500 GeV. This trend will hold up to the sLHC luminosity, corresponding to the mass reach of about 3 TeV shown in fig. 5¹. The discovery reach is shown here, for a specific supersymmetric model, by the wiggly lines labeling the energy and luminosity of the accelerator configuration. The model parameters on the plot’s axis, m_0 and $m_{1/2}$, determine the mass of squarks and gluinos across the plane, as shown by the various equal-mass contours.

At high mass, the search for gluinos and squarks and the study of their final states will not be limited by detector systematics, because of the large amounts of energy released, and statistics will be the dominant limitation in these studies. But even with an early discovery of supersymmetry, with masses in the 1–2 TeV range, the extensive programme of measurements that this will trigger (sparticle masses and couplings) will benefit from the higher sLHC statistics, as discussed in detail in [13]. In this case, however, the lower energies of the jets and of the various final-state objects (leptons, missing transverse energy, b -jets, etc) will be much more sensitive to

¹Above this mass threshold, the production cross section starts falling much more rapidly, due to the vanishing probability of finding quarks and antiquarks inside the proton carrying enough energy for the creation of such massive final states.

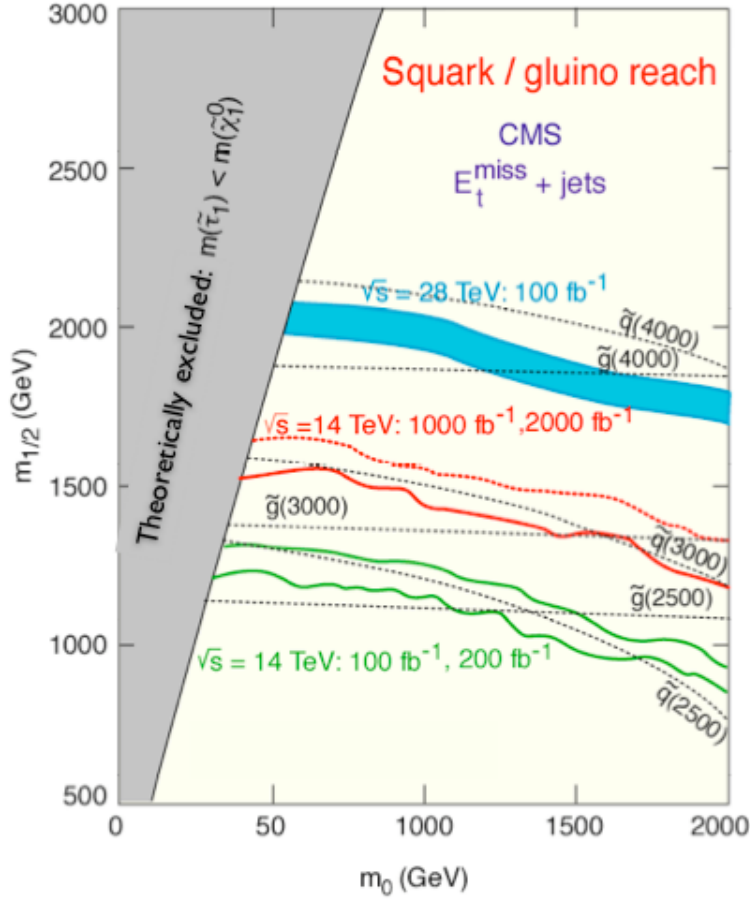


Figure 5. Expected 5σ discovery contours for gluinos and squarks, as a function of the mass parameters m_0 and $m_{1/2}$. The various curves show the potential of the CMS experiment at the standard LHC (for luminosities of 100 fb^{-1} and 200 fb^{-1}), at the sLHC (for 1000 fb^{-1} and 2000 fb^{-1}), and at the DLHC (pp collisions at double-LHC energy, $\sqrt{s} = 28\text{ TeV}$).

the high-luminosity environment of the sLHC, and maintaining excellent detector performance will be the primary concern, as discussed in section 4.1.

2.3 New forces

Figure 6 shows the discovery reach for a new gauge boson Z' , with Standard Model-like couplings, as a function of its mass. With 10 events to claim discovery, the reach improves from 5.3 TeV (LHC, 600 fb^{-1}) to 6.5 TeV (sLHC, 6000 fb^{-1}). Notice that, in spite of the great discovery reach, the ability to extract the values of couplings and to identify the specific nature of the new force is confined to much lower masses, due to the limited statistics. This is shown in fig. 7, in the case of different models for a Z' of 1.5 TeV [32], for Z' decays to $\mu^+\mu^-$ pairs. We show the line shape of the dilepton mass distribution $M(\ell\ell)$, and the leptonic forward-backward asymmetry A_{FB} , as a function of the dimuon invariant mass. Different curves correspond to different Z' couplings as obtained in various potentially interesting models of new gauge symmetries. The points and relative error bars correspond to a specific model, and to the expected statistical uncertainty with an integrated luminosity of 100 fb^{-1} . It was shown in [32] that a clear separation among models can only be achieved for masses up to about 2.5 TeV. A factor of 10 increase in luminosity would extend this reach up to about 3.5 TeV, a mass beyond the reach on any future collider under consideration today.

It is worth adding one more remark. It is unlikely that a Z' will be the only manifestation

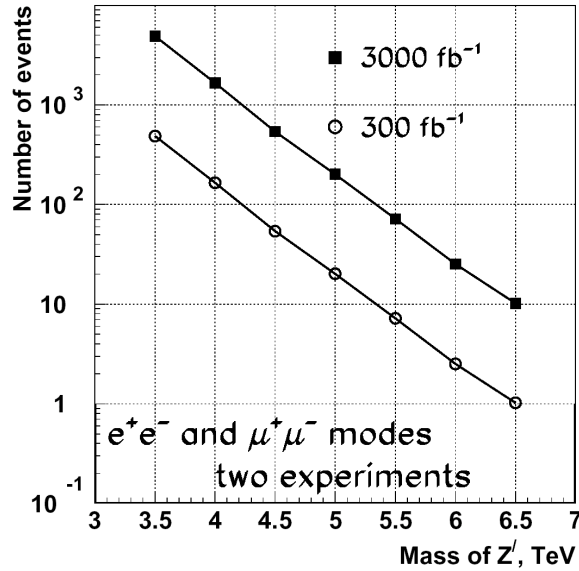


Figure 6. Event rates for a Z' with Standard Model couplings, at the LHC and sLHC.

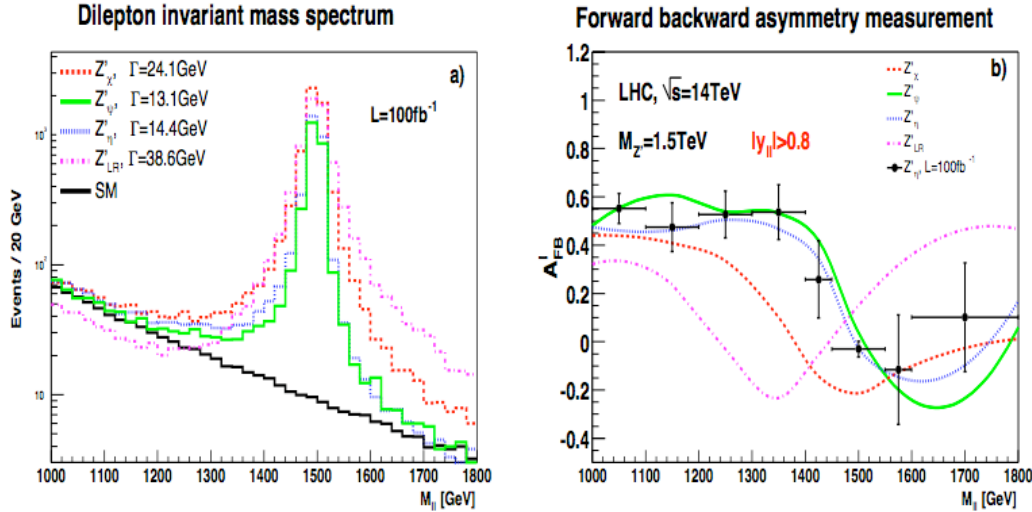


Figure 7. For four models of Z' bosons [32], we show: (a) the spectrum of the dilepton invariant mass ($M(\ell\ell)$) and (b) the forward-backward asymmetry A_{FB} as a function of $M(\ell\ell)$.

of new physics. Additional Z' s occur in most GUT theories, providing, among other things, non-trivial interactions to the otherwise sterile right-handed components of neutrinos. It is well known that the gauge coupling unification predicted by GUT theories is best verified in presence of supersymmetry. The co-existence of supersymmetric particles and of a Z' is therefore a natural conjecture. While the LHC is a powerful machine to produce and detect strongly-coupled supersymmetric particles, the production rates of weakly-coupled states (such as the sleptons, namely the scalar partners of leptons) are rather small, and the backgrounds to their detection are very large. Should these states lie below the threshold for the direct decay of a Z' , their production through the Z' resonance would greatly increase their observability. The study in [33], for example, shows that the discovery reach for sleptons would increase from 170–300 GeV, without a Z' , to over 1 TeV. The Z' mass peak would provide a reference candle for the energy of its decay products, making it possible to accurately determine their mass, even in presence in their decay chain of undetected particles, such as a neutralino, the lightest supersymmetric particle, and a dark matter candidate. In this case, one could directly measure the neutralino mass, and

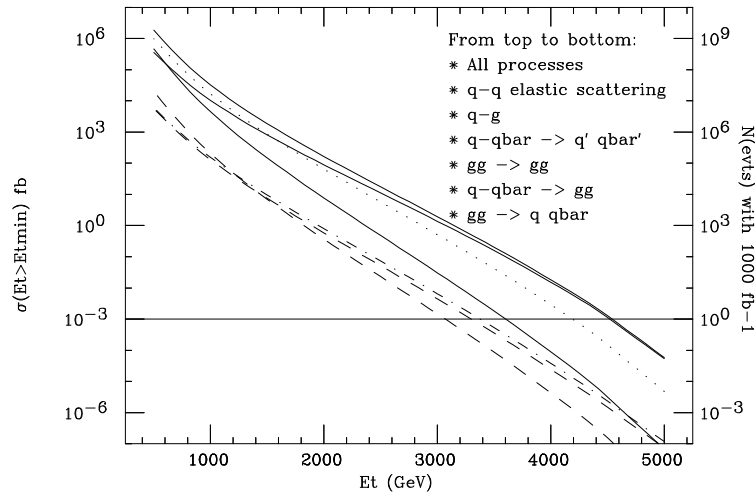


Figure 8. Integrated production cross-section and rates for inclusive central ($|\eta| < 2.5$) jets. The different curves label the contributions of the various initial-state combinations to the total cross-section.

Table 2. The 95% C.L. lower limits that can be obtained on the compositeness scale Λ by using di-jet angular distributions and for various energy/luminosity scenarios [12].

Scenario	14 TeV 300 fb ⁻¹	14 TeV 3000 fb ⁻¹	28 TeV 300 fb ⁻¹	28 TeV 3000 fb ⁻¹
Λ (TeV)	40	60	60	85

see whether it is compatible with the properties of dark matter. Statistics would be the main constrain to pursue a complete study of the spectrum of new particles lying below the Z' . The sLHC could thus become a Z' factory, and acquire many of the advantages so far attributed only to lepton colliders.

2.4 New structure

A tenfold increase in the LHC luminosity should give access to jets of up to $E_T \sim 4.5$ TeV (see Fig. 8), thereby extending the machine kinematic reach for QCD studies by up to 1 TeV. This improved sensitivity should have an impact also on the search for quark sub-structures. Indeed, signals for quark compositeness should reveal themselves in deviations of the high energy part of the jet cross-section from the QCD expectation. The angular distribution of di-jet pairs of large invariant mass provides an independent signature and is less sensitive to systematic effects like possible non-linearities in the calorimeter response. The compositeness scales that can be probed in this way at the LHC and sLHC are summarised in Table 2. For comparison, the potential of a 28 TeV machine is also shown. It can be seen that a tenfold luminosity increase would have an important impact for this physics, comparable to the energy doubling. As these measurements involve only the calorimeters and jets in the TeV range, they can be performed at the sLHC without major detector upgrades. Ability to extend the heavy-flavour tagging to the very high E_T region could however help disentangling the flavour composition of a possible cross-section excess. Only a fraction smaller than few % of the jets with $E_T > 2$ TeV should contain bottom or charm quarks, therefore any indication of a long lifetime component in these jets beyond this level would signal the presence of new physics.

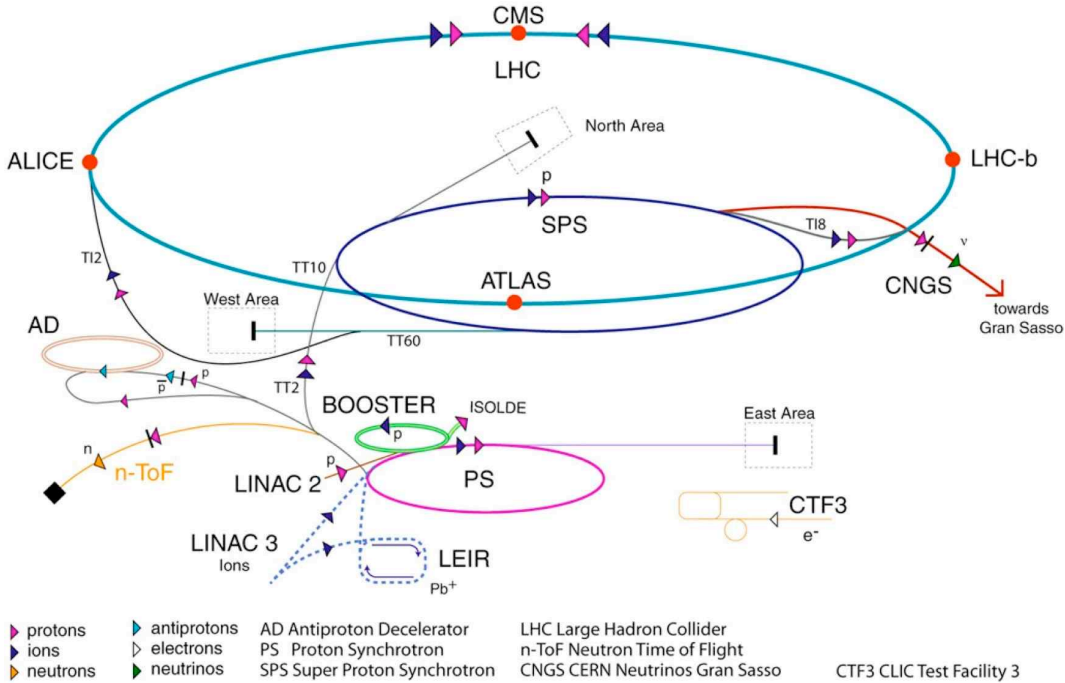


Figure 9. Layout of the full CERN accelerator complex, including all elements of the LHC injector chain. The four interaction regions hosting the main LHC experiments, ALICE, ATLAS, CMS and LHCb, are also shown.

3 The evolution of the accelerator complex

The LHC injector chain is shown in fig. 9. The first stage of the acceleration takes place in the Linac2, a linear accelerator with an output proton energy of 50 MeV. The proton-booster synchrotron (PSB) increases the energy to 1.4 GeV, injecting into the 50-years old proton synchrotron (PS). This accelerates the beam to 26 GeV, and injects into the super proton synchrotron (SPS), out of which 450 GeV protons are eventually injected into the LHC for the start of the ramp up to the nominal energy of 7 TeV. To describe the fundamental constraints and evaluate the technological options available for the luminosity upgrade, it is useful to briefly summarize first some basic notations and notions of accelerator physics.

3.1 The parameters controlling the collider luminosity

As the protons travel around the ring, a sequence of pairs of opposite-polarity (focussing and defocussing) quadrupole magnets prevents the beam from blowing up and confines it within the beampipe. During one full turn, an individual proton oscillates around the ideal circular trajectory a number of times (*betatron oscillations*). To avoid the build up of resonance, this number, called the *tune* (Q), should not be an integer. Any spread or shift of the tune (ΔQ), due for example to the beam-beam interactions as beams cross each other during the collision, should be kept small to avoid hitting these resonances. The transverse size of the envelope of the various trajectories, at a given point s along the ring, is measured by the betatron function $\beta(s)$, a quantity that, point by point, depends on the local optics. Liouville theorem, on the other hand, constrains the possible phase-space evolution of the beam. The associated Liouville invariant is called the beam *emittance*, ϵ . At a fixed momentum, and in an ideal loss-less beam-transport scenario, this is a constant along the ring, while the so-called *normalized emittance*, $\epsilon_n = \beta\gamma\epsilon$ (where $\beta = v/c$ and $\gamma = 1/\sqrt{1-\beta^2}$), is independent of momentum and is a constant across the full beam acceleration and storage path. Its value is defined at the earliest stage of the acceleration process, and will be inherited, with some unavoidable degradation, by the high-

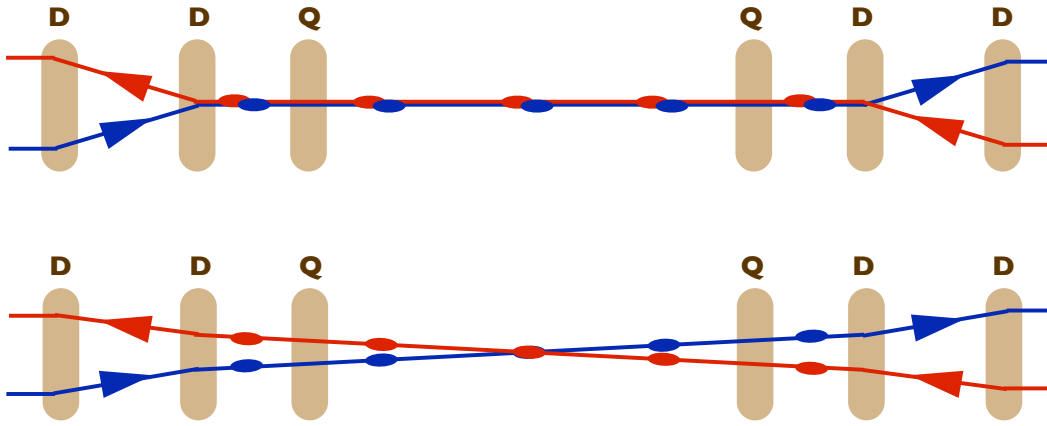


Figure 10. The interaction region at the LHC, with (lower) and without (upper) a crossing angle.

energy components of the accelerator chain. The betatron function and the emittance combine to give the physical transverse size σ of the beam at a point s : $\sigma^2 \sim \epsilon\beta(s)$. This naturally leads to the following relation for the peak collider luminosity:

$$L = \frac{f_r \gamma}{4\pi} \frac{N_b^2 n_b}{\epsilon_n \beta^*} F. \quad (1)$$

Here f_r is the revolution frequency, N_b is the number of protons per bunch, n_b is the number of bunches, β^* is the value of the betatron function at the interaction point (IP), and $F < 1$ is a factor measuring the geometric loss of overlap between two bunches as they cross at a given crossing angle. The luminosity can therefore be increased by increasing the bunch current (N_b), the number of bunches (n_b) and the geometric overlap (F), or by reducing emittance or β^* .

3.1.1 Beam brightness

As mentioned earlier, the normalized emittance is an invariant through the full injector chain. Should the reduced phase-space acceptance of some accelerator element create a bottleneck, the emittance would increase, leading to a degradation of the beam *brightness* $\propto N_b/\epsilon_n$ and of the peak luminosity. At this time, the LHC brightness is limited by the characteristics of the Linac2, of the PSB and of the PS. While these have been shown to provide the brightness required to reach the nominal LHC luminosity of $10^{34} \text{ cm}^{-2}\text{s}^{-1}$, any further luminosity increase based on a boost of the brightness will require an upgrade of these low-energy elements of the injector complex, as will be discussed later. An increase in brightness, on the other hand, leads to an increase in the tune spread due to beam-beam interactions, since $\Delta Q \propto N_b/\epsilon$ for a single head-on collision. To contain the tune shift from multiple collisions due to the short bunch spacing, the present design of the LHC requires collisions to take place at a non-zero crossing angle, as shown in fig. 10. The upper configuration in the figure shows a collision at zero crossing angle. Two dipole magnets on each side of the interaction region (IR) bring the beams collinear from their parallel but separated paths in the respective beampipes; the bunch separation is 7.5 m, and thus each bunch will cross about 30 opposite bunches during the 60 m trajectory across the IR, before being redeflected back into its normal orbit, with a 30-fold increase of the tune shift. To reduce this effect, weak orbit correctors can help bring beams into collision with a small relative angle, as shown in the lower configuration; the beam-beam interactions are suppressed, due to their separation while away from the IP. In this configuration, however, the geometric overlap of the two bunches at the IP is reduced, as shown in fig. 11(a), by a factor $F(\phi) = 1/\sqrt{1+\phi^2}$, where $\phi = \theta_c \sigma_z / (2\sigma_x)$ is the so-called Piwinski angle. Here $\theta_c/2$ is the crossing angle w.r.t. to the horizontal, and $\sigma_{z,x}$ are the longitudinal and transverse bunch dimensions. There is therefore a competition between the need to minimize the tune shift, which approximately decreases with

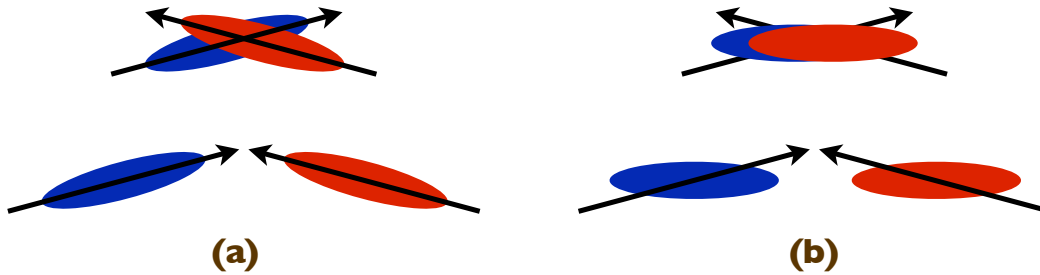


Figure 11. Beam-beam overlap at the IP, in a normal configuration (a) and with a crab crossing (b).

crossing angle by the factor $F(\phi)$, and the desire to increase the bunch intensity, or reduce its transverse size σ_x . This highlights one of the many constraints on the luminosity increase. For nominal LHC operations, the crossing angle is $\theta_c = 285 \mu\text{m}$ and $F \sim 0.8$. A brilliant solution to this problem could come from the development of *crab* RF cavities [34, 35], whose role is to tilt the bunches before they enter the IR, ensuring their total overlap when they cross, as shown in fig. 11(b). So far, crab cavities have only been tested in the KEK e^+e^- collider, and a vigorous R&D is required to develop the technology for the LHC [36].

3.1.2 The number of bunches

The luminosity grows linearly with the number of bunches. The nominal LHC will operate with 2808 bunches per beam, divided into bunch-trains with a bunch-bunch spacing of 25 ns. Increasing the number of bunches while keeping N_b fixed has the great advantage for the experiments of maintaining the same number of interactions within each bunch crossing, thus not increasing the complexity (number of tracks, occupancy in the tracking chambers, energy deposits in the calorimeters, etc) of the final states. Of course more bunches means more frequent interactions, requiring faster read-out electronics, something which however can be achieved in the future. From the accelerator viewpoint, however, an increased number of bunches leads to an increase in the electron-cloud effect. Synchrotron radiation and halo protons hitting the beampipe wall will extract electrons from it, and these electrons, accelerated in the field of the passing-by bunches and hitting themselves the pipe walls, generate a chain reaction where more and more electrons are released. The energy generated by their interaction with the beampipe can increase the temperature of the magnets, leading to a quench, and their presence can furthermore interfere with the main beam causing its disruption. The size of these effects grows rapidly with the bunch frequency. Detailed studies of this effect, in view of the available cooling power and of the beam dynamics, have recently concluded that previous plans to operate at 12.5 ns are unsustainable, and all upgrade schemes are now relying on either the nominal bunch structure, or possibly an increase to a 50 ns spacing, as discussed later.

3.1.3 Reducing β^*

While the overall behaviour of $\beta(s)$ around the full ring is constrained by global stability requirements, like the value of the tune, its value at a specific point depends on the local machine optics. Proper focusing magnets around the IR can therefore reduce β^* , thus increasing the luminosity according to eq. 1. Beam dynamics demands however a price to pay for a beam squeeze at the IP: a greater growth of the beam size before and after the minimum of β^* . The internal aperture of the quadrupole magnets surrounding the IR must match this growth, to prevent the beam hitting their inner surface. An increase in the quadrupole aperture, on the other hand, requires a larger field, in order to maintain the constant field gradient necessary to focus the beam. Alternatively, one should increase the length of the quadrupoles, so that the overall bending stays constant. In both cases, the present focusing quadrupoles surrounding the

IRs of the experiments need to be rebuilt. Notice also that, due to the geometric factor $F(\phi)$, the reduction in β^* , with a constant crossing angle, does not lead to a linear increase in luminosity.

3.2 The LHC luminosity upgrade phases

The overall goal of the upgrade [37] is to increase the integrated luminosity accumulated by the experiments, maintaining their ability to collect good quality data [38]. The pursuit of the highest peak luminosity has therefore to be moderated by considerations of overall efficiency, providing beam lifetimes as long as possible, refill times as short as possible, maximal operational reliability (i.e. short maintenance downtimes), and an optimal experimental environment.

Two main machine parameters characterize the environment within which experiments at the LHC operate: the time between two bunch crossings in the center of a detector, $\Delta\tau_b$, and the average number of pile-up events, i.e. the simultaneous pp collisions that take place in each crossing, N_{int} . $\Delta\tau_b$ sets the time scale for the frequency at which the detector must sample the data, and for the triggering and data acquisition processes. The detector signals are to be read and temporarily stored in a buffer while hardware and software processing analyze the gross features of the event to decide whether it is worth storing, in which case it is finally assembled and written out to tape. Under nominal operations, $\Delta\tau_b = 25\text{ns}$, the reading/processing must be accomplished 40 million times per second. With an average event size of about 1 MB, this means processing 40 PB/s, with the goal of extracting the 100 interesting events, out of 40M, that in one second that can be written to storage for the offline analysis. N_{int} sets the scale of the complexity of the event: each additional pp collision during a bunch crossing contributes to the occupancy of the detector channels, to the processing power needed to trigger, to the size of the event as it is stored. In the offline analysis, these pile-up events will deteriorate the reconstruction of the interesting final states, as discussed in more detail below. A total inelastic pp cross section σ_{pp} of about 60mb, the nominal luminosity of $L=10^{34}\text{ cm}^{-2}\text{s}^{-1}$, and the fraction of the ring populated by bunches ($f = 2808 \times 7.5\text{ m}/27\text{ km}$), give $N_{int} = L \times \sigma_{pp} \times \Delta\tau_b/f \sim 19$. This grows linearly with the instantaneous luminosity.

The present upgrade plan of the LHC [15, 39, 40] is tailored to fulfill a gradual luminosity increase with a sequence of steps, tuned to the construction timescale and complexity of each step, to the need of accommodating the necessary upgrades of the experiments, and the desire to maximize the integrated luminosity delivered by the middle and by the end of the next decade. The effect of these steps is summarized in fig. 12, and is briefly outlined in the following sections.

While the timeline shown here reflects the present planning, it is expected that it will evolve as a function of the actual performance of the LHC during its first one or two years of operation. Likewise, it is still early to have an accurate cost appraisal for the completed project. Nevertheless, current estimates place the cost of the overall luminosity upgrade at a fraction of the LHC cost, below the 1 billion swiss franc threshold. The cost of the upgrade of the SPS and the energy doubling of the LHC, on the other hand, would be significantly higher and approach the scale of the initial LHC cost.

3.2.1 Achieving nominal luminosity

While the LHC injector complex is already capable of delivering the nominal beam brightness, leading to a peak luminosity of $10^{34}\text{ cm}^{-2}\text{s}^{-1}$, it will take some time and some further LHC hardware before this is achieved. The main current limitation is due to the beam collimation system [41]. This system of absorbers, inserted in the beampipe at a close distance from the beam axis and at points far away from the experiments, ensures that protons in the beam halos are captured before their orbit leads them to interact with the beampipe, releasing their energy to the magnets and causing their quench. It is estimated that the present collimation system allows the luminosity to reach approximately $0.3 \times 10^{34}\text{ cm}^{-2}\text{s}^{-1}$. An upgrade is foreseen to allow the nominal luminosity of $10^{34}\text{ cm}^{-2}\text{s}^{-1}$, and beyond. The installation of this system will require a long shut-down of at least 8 months. To maximize the luminosity integrated during the first

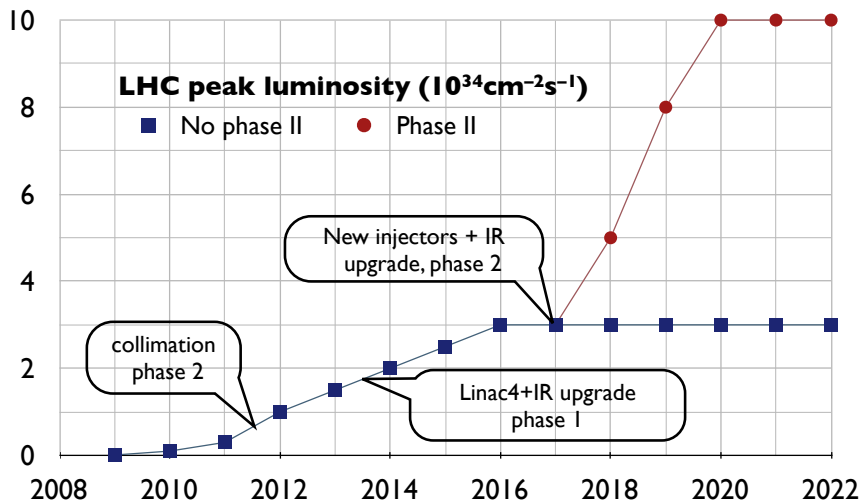


Figure 12. The peak luminosity profile over the next decade, as foreseen by the present upgrade planning.

few years, and in consideration of the time required to master operations at such high luminosity, it is foreseen that this upgrade will take place not before two full years of running (in fig. 12 this is inserted during the 2011-2012 shutdown, labeled as “collimation phase 2”). Once this is done, the LHC luminosity is expected to promptly ramp up to its nominal value, with an expected yearly integral of about 60 fb^{-1} .

3.2.2 The upgrade, phase 1

This phase will rely on the availability of a new linear accelerator, the Linac4, to replace the Linac2, and on the replacement of the IR quadrupoles with greater aperture and greater field ones.

The Linac4, whose construction has started and should be completed by 2014, will raise the injection energy into the PSB from 50 to 160 MeV. The factor of two gain in $\beta\gamma^2$ allows to double the beam intensity at constant tune shift, providing a better match to the space-charge limitations of the PSB. The early stages of the acceleration use an H^- beam, whose two electrons will be eventually stripped off. This step eludes the constraints of Liouville theorem, and reduces the beam emittance. Overall, the improved beam quality will allow to increase N_b from the nominal value of 1.15×10^{11} to $\sim 1.7 \times 10^{11}$, leading to the so-called *ultimate* luminosity of $2.3 \times 10^{34} \text{ cm}^{-2} \text{ s}^{-1}$.

The IRs will need to be upgraded, as discussed in detail in [42]. New quadrupoles [43], built with the same NbTi superconducting cable of the LHC bending dipoles, will allow a reduction of β^* to $\sim 30 \text{ cm}$ in the ATLAS and CMS IRs. With this further improvement, the peak luminosity goal for this phase is of the order of $3 \times 10^{34} \text{ cm}^{-2} \text{ s}^{-1}$, with a yearly integral of 180 fb^{-1} .

A long shutdown of about 8 months will be required for the replacement of the quadrupoles. This is scheduled to take place between the 2013 and 2014 runs. The shutdown should be synchronized with the readiness for installation of important experimental upgrades, such as the trackers.

3.2.3 The upgrade, phase 2

The objective of this second phase, also called the sLHC, is to remove all bottlenecks in the injector chain, allowing the maximum possible beam brightness to reach the LHC, and to improve the overall system reliability, renovating components that, like the PS, are old and require frequent and time consuming repairs. The goal peak luminosity is in the range of $10^{35} \text{ cm}^{-2} \text{ s}^{-1}$. To take full benefit of these beam conditions, a further major modification of the IRs, beyond

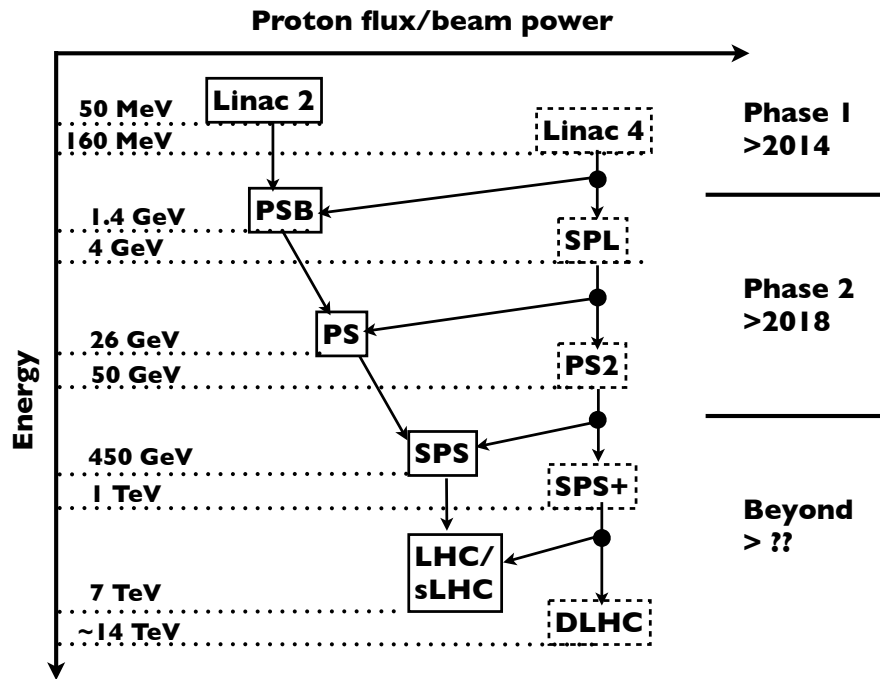


Figure 13. The evolution of the LHC complex upgrade. The arrows show the injection sequence, from lower to higher energy accelerators. The components within dashed boxes on the right-hand side are intended to replace the corresponding elements on the left-hand side. At the completion of phase 2 the chain will link Linac4, SPL and PS2, then injecting into the SPS and finally the LHC.

phase 1, is required, in order to cope with the increase in beam-beam interactions and with the deterioration of the beam lifetime. Furthermore, greater ingenuity is necessary to limit as much as possible the number of interactions per bunch crossing, so that the experiments can take full advantage of the higher interaction rates.

3.2.3.1 The upgrade of the accelerators. The upgrade of the injector complex [40] is sketched in fig. 13. In addition to the Linac4, which will already be operating since phase 1, the upgrade calls for a replacement of both the PSB and the PS. The PSB would be replaced by a low-power superconducting linear accelerator (SPL [44]), increasing the injection energy into the PS from 1.4 to 4 GeV and greatly reducing the filling time. The increase in output energy of the SPL will allow to increase also the output energy of the next step in the chain, where a new synchrotron, the PS2, will replace the PS. The PS2 will deliver protons to the SPS at 50 GeV, well above the 23 GeV transition energy of the SPS, easing the handling of higher intensities. Injection into the SPS at 50 GeV will reduce the space-charge tune spread, to allow the bunch intensity to reach $N_b \sim 3.6 \times 10^{11}$ for 25 ns bunch separation (and up to $N_b \sim 5.5 \times 10^{11}$ with 50 ns bunches). Higher energy also gives smaller emittance, and less beam losses at injection. Shorter injection and acceleration times, finally, reduce the filling time, with a greater operational efficiency.

3.2.3.2 The upgrade of the interaction regions. This great increase in beam intensity needs a complete redesign of the IRs. Four schemes are presently under consideration [15, 39]: early separation (ES) of the beams, full crab crossing (FCC), large Piwinski angle (LPA) and low emittance (LE). In the ES scheme additional small superconducting dipoles are positioned on either side of the IP, residing within the detectors. This allows to keep the bunches separated until these final dipoles, reducing the tune-shift. Small-angle crab cavities, located outside the quadrupoles, would allow for a total overlap at the collision. The FCC scheme solely relies on crab cavities to maximize the bunch overlap. The LE scheme provides much thinner bunches, at

Table 3. Main parameters of the proposed schemes for the IRs. $L_{eff}^{10(5)hr}$ represents the effective luminosity, accounting for a LHC refilling time at the end of each store of 10 (5) hours.

Parameter	Nominal	Ultimate	ES	FCC	LE	LPA
emittance $\epsilon[\mu\text{m}]$	3.75	3.75	3.75	3.75	1.0	3.75
$N_b [10^{11}]$	1.15	1.7	1.7	1.7	1.7	4.9
bunch spacing [ns]	25	25	25	25	25	50
β^* [cm]	55	50	8	8	10	25
$\theta_c [\mu\text{rad}]$	285	315	0	0	311	381
peak L [$10^{34} \text{ cm}^{-2}\text{s}^{-1}$]	1	2.3	15.5	15.5	16.3	10.7
$\langle \text{events/crossing} \rangle$	19	44	294	294	309	403
L lifetime (τ_L [hr])	22	14	2.2	2.2	2.0	4.5
$L_{eff}^{10hr} [10^{34} \text{ cm}^{-2}\text{s}^{-1}]$	0.46	0.91	2.4	2.4	2.5	2.5
$L_{eff}^{5hr} [10^{34} \text{ cm}^{-2}\text{s}^{-1}]$	0.56	1.15	3.6	3.6	3.7	3.5

a cost of a larger geometric loss. The LPA scheme allows for much more intense beams, requiring a longer bunch spacing of 50 ns and a larger crossing angle, limiting the tune shift with a flat beam profile. Long-range beam-beam interactions need to be screened with compensating wires, to reduce the tune spread. In this scheme, lower-intensity bunches separated by 25 ns from the primary ones would have to be inserted in order to allow collisions in LHCb, whose position along the ring is out of synch with the collision points of the 50 ns bunches.

In general, more performing quadrupoles, built of Nb₃Sn cable, will be required, to allow for the reduction of β^* envisaged in most schemes, and for the greater aperture needed in the LPA scheme. R&D for these new-generation magnets is underway [43].

The value of the main parameters discussed so far, for the four upgrade options and for the pre-sLHC phases, is shown in table 3. In particular, notice the important decrease in the luminosity lifetime with all sLHC schemes. The drop in luminosity is proportional to the increase in interaction rate, and is just due to the loss of protons due to the collisions. With a bunch-bunch crossing each 25 ns, 300 pp collisions at each crossing, and two active experiments (ATLAS and CMS), a number of the order of 10^{14} p/hr is disappearing, out of a total of about 5×10^{14} stored in the initial beam! Under these conditions, it is critical to reduce as much as possible the time required to prepare and refill the LHC for a new store. The envisaged turaround times range from a conservative 10 hours, to a goal of 5 hours; the impact of this dead time on the effective luminosity is shown in the last two rows of the table, and the expected luminosity profiles, for a 5-hour turnaround, is displayed in upper left corner of fig. 14.

The upper right plot of fig. 14 shows the average number of expected pp interactions, N_{int} , taking place during each crossing. These numbers, well in excess of 100, should be compared with $N_{int} \sim 20$ obtained at the nominal luminosity of $10^{34} \text{ cm}^{-2}\text{s}^{-1}$, a number already putting great strain on the detector performance. It has been noticed that proper manipulations of the beam parameters during a single store could level out the luminosity profile, maintaining the same average luminosity, and providing much more stable and sustainable conditions for the experiments. The result is shown in the lower set of plots of fig. 14.

Luminosity leveling can be achieved by having a larger value of β^* , or a larger crossing/crab angle, early on in the store, and reducing them as the beam intensity diminishes during the store. It is clear that it will provide one of the most powerful tools to enhance the benefits of the luminosity upgrade, and it is therefore an essential part of the future planning for the sLHC!

3.2.4 Beyond phase 2

The most natural further upgrade of the LHC, beyond phase 2, is the energy increase, possibly by a factor of at least 2. The challenge, magnitude and cost of this effort are significantly larger than the sLHC [14]. The precondition for its feasibility is the development and industrialization of bending dipoles with fields in the range of 15-20 T [43, 45]. This can be achieved in principle with Nb₃Sn superconducting cables, such as those being developed for the phase 2 quadrupoles. Yet higher fields, around 24 T, or centre-of-mass energies around 40 TeV, could be achieved with inner-core windings of Bi-2212 [46]. Aside from the development of the technology needed to

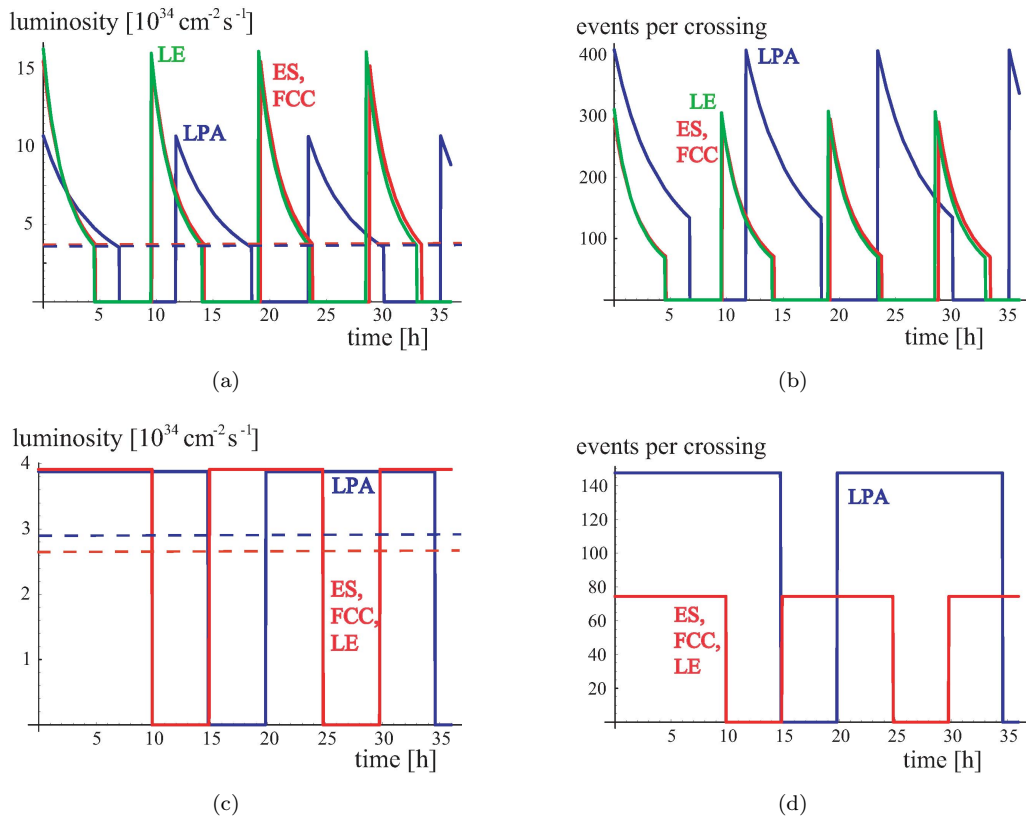


Figure 14. Luminosity profile (left side) and number of interactions per bunch crossing (right side) for the four IR upgrade options. The upper set of plots corresponds to running operations at fixed beam parameters, the lower set shows the effect of luminosity leveling.

produce cables of the required quality (sufficient current density, strain and radiation tolerance, etc.) and length (multi-km!), a major difficulty of these dipoles will be the management of the immense magnetic forces, acting both on the overall structure of the magnets, and on their internal components. The timescale for these developments and for more conclusive statements about the technological feasibility and cost of a DLHC (the *Double-LHC*) is estimated to be no less than 10 years. It has to be added that the DLHC requires also an energy upgrade of the SPS, the SPS+, to boost the injection energy to 1 TeV.

4 The experimental upgrades

Three key considerations define the needs of the detector upgrades on the way towards the sLHC and beyond [38]: *(i)* some components will need to be replaced due to the damage caused by radiation even before the start of the sLHC; *(ii)* some components will not be operable in the harsh high-luminosity environment of the sLHC; *(iii)* the performance of some of the existing components will not be adequate, at the sLHC, to fulfill the physics needs. These issues will be reviewed in this section, starting from the physics requirements.

4.1 Physics performance

The criteria for the physics performance of the experiments are driven by the nature of the observables that will be of interest at the sLHC. In turn, these are defined by the research programme that will emerge after the first few years of data taking, once the nature of the new phenomena of interest will be more clearly defined.

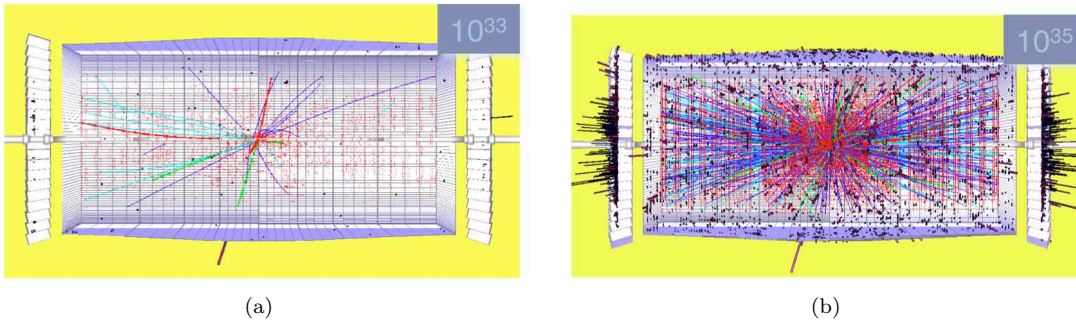


Figure 15. The same event, as seen at $10^{33} \text{ cm}^{-2}\text{s}^{-1}$ (left) and at $10^{35} \text{ cm}^{-2}\text{s}^{-1}$, with the inclusion of $O(100)$ additional pp interactions during the same bunch crossing.

As mentioned above, the main impact of running at high luminosity will be the increased number of pile-up events, namely the additional pp interactions taking place during a single bunch crossing. A dramatic picture of what this entails is shown in fig. 15, where the same event appears displayed in the presence of the low pile-up of collisions at $10^{33} \text{ cm}^{-2}\text{s}^{-1}$, and of the many hundreds of additional events occurring at $10^{35} \text{ cm}^{-2}\text{s}^{-1}$.

The impact of these pile-up events will be twofold. On one side, many more tracks will be present. This will greatly increase the number of hits in the tracking detectors, especially at small radius, where low-momentum particles curling up in the magnetic field cross the trackers many times. With the increase in occupancy, reconstructing tracks becomes more and more difficult. The chances to wrongly assign hits will increase the number of fake tracks, and this extra noise may prevent the reconstruction of good tracks. The ability to reconstruct displaced vertices will also deteriorate, with a reduced efficiency to tag b quarks and τ leptons, and a larger rate of fake tags. More hits will also mean much more computing time required to perform the pattern recognition, affecting both the performance of tracking triggers, and of the offline analysis. Most of these issues can be addressed by increasing the granularity of the detectors, e.g. through a more extended use of pixels even at large radii. This would reduce the occupancy, avoid overlaps of signals, and improve the pattern recognition. The penalty is a large increase in the number of electronics channels, extra heat-load to be removed, and likely an increase in the amount of detector material, which deteriorates the momentum and energy measurements because of the increased interactions of the primary particles.

The other consequence of greater pile-up is the presence of much more energy within the cones used to reconstruct jets. The extended transverse size of a jet is determined by physics, and an increased granularity of the calorimeters, contrary to the case of the trackers, would not help. The jets from the decay of a top quark, for example, would collect a large amount of spurious energy from the pile-up events. Even if their average contribution can be subtracted, event-by-event fluctuations cannot be disentangled, causing a significant deterioration in the jet energy resolution. The reconstruction of a sharp invariant-mass peak in a two-jet final state would therefore be harder, and the significance of the peak signal on top of a large continuum background reduced. Furthermore, electron identification and trigger efficiency would deteriorate, due to the larger amount of energy surrounding an otherwise isolated electron, which will reduce the effectiveness of the usual isolation criteria. And, last but not least, the large number of additional events can contribute both to the presence of extra objects (such as jets or leptons), and of missing transverse energy, due to energy fluctuations and to undetected large-transverse-momentum particles emitted at small angle. The additional central jets could jeopardize the use of jet-vetoing in the study of Higgs production by vector-boson fusion, as discussed in section 2.1.3, and the high rates of forward energy could likewise compromise the forward jet tagging required by these same studies.

The effect of the above considerations can be qualitatively assessed by looking at a possible reference process, the production and decay of a squark-gluino pair sketched in fig. 16. With four

4.2.2 The transition to phase 2

In view of the four options currently under consideration for the accelerator phase 2 upgrade, and of the relative impact on detector performance, the preference of the experiments goes to the full-crab-cavity scheme with luminosity leveling. In comparison, the LPA scheme has a pile-up twice as large as that of the other schemes, while the ES scheme forces the presence of accelerator elements inside the detectors, compromising, among other things, the forward jet-tagging performance. Given the still uncertain outcome of the study of the accelerator options, the experiments are nevertheless exploring upgrade options capable of getting the best out of each possible running scenario. In addition to a vigorous R&D effort on many fronts, new software tools are also being developed to reliably model the performance in presence of up to 400 pile-up events.

Some of the key issues for these upgrades are outlined below. A more complete discussion can be found in [12, 38].

4.2.2.1 Tracking. The current inner trackers of ATLAS and CMS will only survive approximately 700 fb^{-1} , and can operate at best not above $3 \times 10^{34} \text{ cm}^{-2}\text{s}^{-1}$. New tracking detectors, likely exploiting new technologies such as the use of diamond, will therefore be needed by the start of the sLHC.

The detector granularity will be increased to keep occupancy at the 1-2% level for an efficient pattern recognition. This can be achieved by reducing pixel size, strip dimensions for silicon counters, and by adding more detector layers to increase the number of precision points per track. This should be done with the constraint of handling the increased number of channels, the relative heat-load, and trying to preserve or reduce the material amount, to minimize the interactions of photons and electrons as they cross the trackers. Several different technology options and layouts are under consideration.

4.2.2.2 Muons. The muon systems of ATLAS and CMS are built with a large safety factor, needed to accommodate the still unknown amount of backgrounds expected at the LHC. If the current estimates of backgrounds are correct, they could in fact maintain their performance even at the sLHC, at least in the central rapidity region. Options to reduce the background levels include, for ATLAS, a replacement of the beampipe with a more transparent one in beryllium, along the full 50m of the detector. A replacement for the most forward components, nevertheless, is being considered.

4.2.2.3 Calorimetry. The central calorimeters are the most massive components of the detectors. Their replacement is not an option. Fortunately this is not required, since, as mentioned earlier, no improvement in their granularity or energy resolution can compensate for the higher pile-up environment. The electronics and power supplies will nevertheless be changed, due to the radiation damage and to improve the flexibility of the triggers.

The high radiation doses and heat deposition, on the other hand, will require a major rework on the ATLAS forward liquid-argon calorimeters. This may call for a replacement of the technology, or for better active shielding. The effect on muon backgrounds of the presence of new large-aperture quadrupoles in the final focus, and their shielding, will also need to be reviewed.

4.2.2.4 Trigger and data acquisition. The need is to keep trigger-accept rates constant at each level. Relative to the current systems, this means rejecting 10 times as many events, and writing 10 times as many bytes, due to the increased size of the events in presence of large pile-up. More efficient triggers need to be designed, capable in particular of sorting through the massive upfront data flow. The emphasis will therefore be on the first trigger levels, where one

may need to incorporate tracking information, to supplement the reduced rejection power of muon and calorimeter triggers, and to maintain acceptable efficiency and purity for electrons, affected by the degradation of isolation criteria at $10^{35} \text{ cm}^{-2}\text{s}^{-1}$.

4.2.2.5 General remarks. The upgrade of the LHC experiments will require major R&D and construction work, with a likely timeline of at least 6-7 years for construction and integration. The planning has to assume the worse possible scenarios in terms of pile-up and radiation environment. While the financial green light for this new enterprise will probably take a few years and will be tuned to the first LHC discoveries, the detector community has to act now, preparing technology, making choices, testing prototypes and going deeply in the engineering design.

The definition of the scope of the phase 2 upgrades will develop in parallel with the planning of the IRs upgrades and with the extensive R&D programme underway. It is anticipated to converge towards technical design reports by 2012, together with the complete definition and approval of the accelerator project.

The goal is to keep the length of the required shutdown to no more than 18 months, to limit to 1 year the loss of beam, and consistent with the time required in the LHC planning for the IRs changes.

5 Outlook and conclusions

Whatever is discovered at the LHC, it will define the research direction for the future. For example, if supersymmetry is seen, the key problem of the field will become to understand the origin of supersymmetry breaking, like today we are confronted with the problem of EWSB. The first step in this direction will be the measurement of the spectra, mixings and couplings of the new particles. In the case of the Standard Model, the complete determination of its parameters has taken about 30 years, and it would be naïve to expect a shorter time scale for the full exploration of what will be revealed by the LHC.

Hadron accelerators can enjoy great scientific longevity, as shown by the Fermilab's Tevatron. Its first physics data were taken in 1987; the first major discovery, the top quark, came in 1994; crucial results such as the measurement of the W mass and the first evidence of CP violation in the B^0 system arrived few years later. After a 5-year upgrade shut-down, the CDF and D0 experiments continued their discovery path, with the first observation of B_s mixing in 2006, an accurate measurement of $D^0 - \bar{D}^0$ mixing in 2007, a determination of the top mass with accuracy below 1% in 2008, and finally reaching, more than 20 years after start-up, sensitivity to the existence of a Standard Model Higgs boson below ~ 170 GeV. There is no reason to believe that the LHC should not deliver significant discoveries and measurements for at least as long.

The complete exploration of the new landscapes unveiled by the LHC will certainly require additional elements in the experimental programme, in parallel and beyond the (s)LHC [47, 48]. In addition to the development of high-energy lepton colliders [49, 50], which will improve the measurement accuracy and sensitivity of the LHC, this programme includes lower-energy but high-intensity experiments, focused on the flavour sector of particle physics, notably in the areas of neutrino physics [19], rare K decays and B physics [51], flavour-violation in the charged lepton sector and electric dipole moments [52]. The possibility to address several of these lower-energy programmes with experiments driven by the beams of the renewed LHC injector complex [53, 54] is an added value to an upgrade of the LHC, which adds significant physics motivations to its realization.

While several efforts are underway to define plans for future accelerators, it is necessary and timely that the full potential of the LHC be considered and evaluated. The LHC accelerator complex provides a unique infrastructure, whose upgrades might turn out to be the most effective

way to extend the knowledge about particle physics in the decades to come. The cost of these upgrades, and their technological challenge, might turn out to be as demanding as those of competing projects. On the other hand, the exploratory potential of a high-energy hadronic collider is unchallenged, and all efforts should be made to ensure that no stone is left unturned when evaluating how far the LHC can take us in unveiling the ultimate secrets of nature. In addition to the luminosity upgrade, which was the focus of this review, this path should include the consideration of an energy upgrade, leading to at least a doubling of the center of mass energy. The current technology provides a natural time ordering to these two upgrades, with the luminosity one being closer in reach. The path towards the luminosity upgrade of the LHC is determined by important compromises, characterizing the impact that each technological choice on the accelerator side has on the detector performance, and viceversa. The weight to assign to each element depends on the specific focus of the physics programme, something that may only become entirely clear after the first few years of LHC operations. A target the whole community is eagerly waiting for.

Acknowledgements

To prepare this review I benefited from the input, implicit or explicit, of many colleagues with whom I discussed these issues over the years, as well as of the lecturers of the recent CERN Academic Training course on *Scenarios and Technological Challenges for a LHC Luminosity Upgrade*, wisely planned and well organized by S. Gobba and J.-P. Koutchouk. A likely incomplete list of those I should like to thank includes: R. Assmann, J. Ellis, L. Evans, R. Garoby, F. Gianotti, N. Hesse, J. Nash, M. Nessi, G. Rolandi, L. Rossi, F. Ruggiero, W. Scandale, J. Tuckmantel, J. Virdee, F. Zimmermann.

This work is supported in part by the European Communitys Marie- Curie Research Training Network HEPTOOLS under contract MRTN-CT-2006-035505.

References

- [1] S. L. Glashow, *Partial Symmetries Of Weak Interactions*, Nucl. Phys. **22** (1961) 579. A. Salam and J. C. Ward, *Electromagnetic and weak interactions*, Phys. Lett. **13** (1964) 168. S. Weinberg, *A Model Of Leptons*, Phys. Rev. Lett. **19** (1967) 1264.
- [2] P. W. Higgs, *Broken symmetries, massless particles and gauge fields*, Phys. Lett. **12** (1964) 132. F. Englert and R. Brout, *Broken symmetry and the mass of gauge vector mesons*, Phys. Rev. Lett. **13** (1964) 321. G. S. Guralnik, C. R. Hagen and T. W. B. Kibble, *Global conservation laws and massless particles*, Phys. Rev. Lett. **13** (1964) 585.
- [3] G. 't Hooft, *Renormalization Of Massless Yang-Mills Fields*, Nucl. Phys. B **33** (1971) 173. G. 't Hooft and M. J. G. Veltman, *Regularization And Renormalization Of Gauge Fields*, Nucl. Phys. B **44**, 189 (1972).
- [4] M. Kobayashi and T. Maskawa, *CP Violation In The Renormalizable Theory Of Weak Interaction*, Prog. Theor. Phys. **49** (1973) 652.
- [5] ALEPH Collaboration, CDF Collaboration, D0 Collaboration, DELPHI Collaboration, L3 Collaboration, OPAL Collaboration, SLD Collaboration, LEP Electroweak Working Group, Tevatron Electroweak Working Group SLD Electroweak Working Group and Heavy Flavour Group, *Precision Electroweak Measurements and Constraints on the Standard Model*, arXiv:0811.4682 [hep-ex].
- [6] J. Erler and P. Langacker, *Electroweak model and constraints on new physics*, in [7].
- [7] C. Amsler *et al.* [Particle Data Group], *Review of particle physics*, Phys. Lett. B **667** (2008) 1.
- [8] [CDF Collaboration and D0 Collaboration], *Combined CDF and DZero Upper Limits on Standard Model Higgs-Boson Production with up to 4.2 fb⁻¹ of Data*, arXiv:0903.4001 [hep-ex].
- [9] G. Aad *et al.* [ATLAS Collaboration], *The ATLAS Experiment at the CERN Large Hadron Collider*, JINST **3** (2008) S08003.
- [10] The CMS collaboration, *Physics Technical Design Reports*, at <http://cmsdoc.cern.ch/cms/cpt/tdr/index.html>.
- [11] J. J. Blaising *et al.*, *Potential LHC contributions to Europe's future strategy at the high-energy frontier*, available at <http://cern.ch/council-strategygroup/BB2/contributions/Blaising2.pdf>.
- [12] F. Gianotti and M. L. Mangano, *LHC physics: The first one-two year(s)*, arXiv:hep-ph/0504221.
- [13] F. Gianotti *et al.*, *Physics potential and experimental challenges of the LHC luminosity upgrade*, Eur. Phys. J. C **39** (2005) 293 [arXiv:hep-ph/0204087].
- [14] O. S. Bruning *et al.*, *LHC luminosity and energy upgrade: A feasibility study*, available at <http://cdsweb.cern.ch/record/601847/>.
- [15] W. Scandale and F. Zimmermann, *Scenarios for sLHC and vLHC*, 18th Hadron Collider Physics Symposium 2007 (HCP 2007) 20-26 May 2007, La Biodola, Isola d'Elba, Italy. Published in Nucl.Phys.Proc.Suppl.177-178:207-211,2008.
- [16] *Scenarios and Technological Challenges for a LHC Luminosity Upgrade*, 8 lectures delivered as part of

- CERN's 2009 Academic Training programme, S. Gobba and J.-P. Koutchouk eds., 8-12 June 2009, available at <http://indico.cern.ch/conferenceDisplay.py?confId=55041>.
- [17] R. Barbieri, *Searching for new physics at future accelerators*, arXiv:hep-ph/0410223.
- [18] M. Drees and G. Gerbier, *Dark matter*, in [7].
- [19] R. N. Mohapatra *et al.*, *Theory of neutrinos: A white paper*, Rept. Prog. Phys. **70** (2007) 1757 [arXiv:hep-ph/0510213].
- [20] J. Wess and B. Zumino, Phys. Lett. B **49**, 52 (1974).
- [21] G. L. Kane, Contemp. Phys. **41** (2000) 359.
- [22] The ALICE collaboration, *Technical Design Reports*, at <http://aliceinfo.cern.ch/Collaboration/Documents/TDR/index.html>
- [23] The LHCb collaboration, *Technical Design Reports*, at <http://cern.ch/lhcb/TDR/TDR.htm>.
- [24] The TOTEM experiment, see <http://cern.ch/Totem/>.
- [25] The LHCf experiment, see <http://www.stelab.nagoya-u.ac.jp/LHCf/>.
- [26] G. F. Giudice, C. Grojean, A. Pomarol and R. Rattazzi, *The Strongly-Interacting Light Higgs*, JHEP **0706**, 045 (2007) [arXiv:hep-ph/0703164].
- [27] D. Zeppenfeld, R. Kinnunen, A. Nikitenko and E. Richter-Was, *Measuring Higgs boson couplings at the LHC*, Phys. Rev. D **62** (2000) 013009.
- [28] T. Han and B. McElrath, *$h \rightarrow \mu\mu + \mu\mu$ via gluon fusion at the LHC*, hep-ph/0201023.
- [29] M. S. Chanowitz and M. K. Gaillard, *The Tev Physics Of Strongly Interacting W's And Z's*, Nucl. Phys. B **261**, 379 (1985).
- [30] A. Dobado, M. J. Herrero, J. R. Pelaez and E. Ruiz Morales, *LHC sensitivity to the resonance spectrum of a minimal strongly interacting electroweak symmetry breaking sector*, Phys. Rev. D **62**, 055011 (2000) [arXiv:hep-ph/9912224].
- [31] G. Weiglein *et al.* [LHC/LC Study Group], Phys. Rept. **426**, 47 (2006) [arXiv:hep-ph/0410364].
- [32] M. Dittmar, A. S. Nicollerat and A. Djouadi, *Z' studies at the LHC: An update*, Phys. Lett. B **583** (2004) 111 [arXiv:hep-ph/0307020].
- [33] M. Baumgart, T. Hartman, C. Kilic and L. T. Wang, *Discovery and measurement of sleptons, binos, and winos with a Z'*, JHEP **0711** (2007) 084 [arXiv:hep-ph/0608172].
- [34] R. B. Palmer, *Energy scaling, crab crossing and the pair problem*, in the Proceedings of 1988 DPF Summer Study on High-energy Physics in the 1990s (Snowmass 88), Snowmass, Colorado, 27 Jun - 15 Jul 1988, pp 613-619.
- [35] K. Oide and K. Yokoya, *The crab crossing scheme for storage ring colliders*, Phys. Rev. A **40** (1989) 315.
- [36] J. Tuckmantel, *Crab cavities*, in [16] and available at <http://indico.cern.ch/conferenceDisplay.py?confId=55044>.
- [37] L. Evans, *Introduction to the LHC upgrade programme*, in [16] and available at <http://indico.cern.ch/conferenceDisplay.py?confId=55041>.
- [38] M. Nessi, *The Detector Upgrade and the Requirements on the Upgrade Scenarios*, in [16] and available at <http://indico.cern.ch/conferenceDisplay.py?confId=55042>.
- [39] F. Zimmermann, *Scenarios for the LHC Luminosity Upgrade*, in [16] and available at <http://indico.cern.ch/conferenceDisplay.py?confId=55043>.
- [40] R. Garoby, *Upgrade of the Injector Chain*, in [16] and available at <http://indico.cern.ch/conferenceDisplay.py?confId=55045>.
- [41] R. Assmann, *Collimation and Machine Protection*, in [16] and available at <http://indico.cern.ch/conferenceDisplay.py?confId=55045>.
- [42] V. Baglin *et al.*, *Conceptual Design of the LHC Interaction Region Upgrade — Phase-I*, LHC Project Report 1163. Available at <http://cdsweb.cern.ch/record/1141043/>.
- [43] L. Rossi, *Magnet technology*, in [16] and available at <http://indico.cern.ch/conferenceDisplay.py?confId=55044>.
- [44] R. Garoby, *The potential of the SPL at CERN*. Available at <http://cdsweb.cern.ch/record/815734/>.
- [45] Proceedings of the Workshop on Accelerator Magnet Superconductors, *Design and Optimization*, CERN-2009-001, E. Todesco (ed.), 19-23 May 2008, CERN, Geneva, Switzerland, available at <http://cdsweb.cern.ch/record/1162820>.
- [46] P. M. McIntyre and A. Sattarov, *On the feasibility of a tripler upgrade for LHC*, in the Proceedings of Particle Accelerator Conference (PAC 05), Knoxville, Tennessee, 16-20 May 2005, pp 634.
- [47] T. Akesson *et al.*, *Towards the European strategy for particle physics: The briefing book*, Eur. Phys. J. C **51** (2007) 421 [arXiv:hep-ph/0609216].
- [48] M. L. Mangano, *Physics At The High Intensity Frontier*, Nucl. Phys. Proc. Suppl. **154** (2006) 5.
- [49] G. Aarons *et al.* [ILC Collaboration], *International Linear Collider Reference Design Report Volume 2: PHYSICS AT THE ILC*, arXiv:0709.1893 [hep-ph].
- [50] E. Accomando *et al.* [CLIC Physics Working Group], *Physics at the CLIC multi-TeV linear collider*, arXiv:hep-ph/0412251.
- [51] M. Artuso *et al.*, *B, D and K decays*, Eur. Phys. J. C **57**, 309 (2008) [arXiv:0801.1833 [hep-ph]].
- [52] M. Raidal *et al.*, *Flavour physics of leptons and dipole moments*, Eur. Phys. J. C **57** (2008) 13 [arXiv:0801.1826 [hep-ph]].
- [53] A. Blondel *et al.*, *Physics opportunities with future proton accelerators at CERN*, arXiv:hep-ph/0609102.
- [54] M. Benedikt *et al.*, *Potential for neutrino and radioactive beam physics of the foreseen upgrades of the CERN accelerators*, available at <http://cdsweb.cern.ch/record/946249>.